

1 Lineage tracing of the bivalve shell field with special interest in the descendants  
2 of the 2d blastomere

3

4 Masakuni Mohri, Naoki Hashimoto and Hiroshi Wada\*

5 Graduate School of Life and Environmental Sciences, University of Tsukuba,

6 Tsukuba 305-8572, Japan

7

8 \*Author for Correspondence;

9 Tel&Fax:+81-29-853-4671

10 e-mail:[hwada@biol.tsukuba.ac.jp](mailto:hwada@biol.tsukuba.ac.jp)

11

12

13

14

15

16

17

18 **Abstract**

19 By evolving bilaterally separated shell plates, bivalves acquired a unique body  
20 plan in which their soft tissues are completely protected by hard shell plates. In  
21 this unique body plan, mobility between the separated shell plates is provided by  
22 novel structures such as a ligament and adductor muscles. As a first step toward  
23 understanding how the bivalve body plan was established, we investigated the  
24 development of the separated shell plates and ligament. Over 100 years ago it  
25 was hypothesized that the development of separated shell plates is tightly linked  
26 with the unique cell cleavage (division) pattern of bivalves during development,  
27 wherein each bilateral daughter cell of the 2d descendant, 2d<sup>1121</sup>, develops into  
28 one of the bilateral shell fields. In the present study we tested this hypothesis by  
29 tracing the cell lineages of the Japanese purple mussel *Septifer virgatus*.  
30 Although the shell fields were found to be exclusively derived from the bilateral  
31 descendant cells of 2d: 2d<sup>11211</sup> and 2d<sup>11212</sup>, the descendants of these cells were not  
32 restricted to shell fields alone, nor were they confined to the left or right side of  
33 the shell field based on their lineage. Our study demonstrated that ligament cells  
34 are also derived from 2d<sup>11211</sup> and 2d<sup>11212</sup> indicating that the ligament cells

35 emerged as a subpopulation of shell field cells. This also suggests that the  
36 establishment of the novel developmental system for the ligament cells was  
37 critical for the evolution of the unique bodyplan of bivalves.  
38

39

## 40 **1.INTRODUCTION**

41 Molluscs share several characteristic features, such as calcareous shells (or  
42 spicules) and a muscular foot. However, their body plans are highly variable, as  
43 demonstrated by the differences between the worm-like, shell-less Aplacophora  
44 and the highly motile Cephalopoda. With the development of bilaterally  
45 separated shell plates, bivalves evolved a unique body plan in which their soft  
46 tissue is completely protected by hard shell plates. The muscle system was  
47 rearranged to accommodate the evolution of this shell plate morphology, resulting  
48 in another evolutionary novelty, the adductor muscle, which controls the opening  
49 and closing of the shell plates. Determining how this unique bivalve body plan  
50 was achieved through the coordinated evolution of shell plate morphology and  
51 muscles is challenging. To address this question we first investigated how the  
52 bilaterally separated shell plates developed through the modification of shell  
53 development.

54           Over 100 years ago Lillie and Meisenheimer [1, 2] reported a pattern of  
55 spiral cleavage in bivalves. Most molluscan species exhibit spiral cleavage  
56 wherein the animal blastomeres are smaller than the vegetal blastomeres.

57 However, the dorsal vegetal blastomeres (1D) produce a larger animal blastomere  
58 (2d) in bivalves from the eight-cell stage to the 16-cell stage[3, 4]. This animal  
59 blastomere is thought to be the precursor of the shell field cells, which underlie  
60 shell plates[1, 2]. After four rounds of asymmetric cleavage, the largest  
61 blastomere ( $2d^{1121}$ ) exhibits bilateral cleavage (Figure 1a-e), and the bilateral  
62 daughter cells were suggested to differentiate into the left and right shell field  
63 cells of their respective side[1]. This hypothesis suggests that development of the  
64 novel shell plate morphology was driven by a modification of the early cleavage  
65 pattern. However, it was based solely on microscopic observations and  
66 experimental validation is required through direct cell lineage tracing.

67           It is also notable that bivalves show a stereotypic pattern of spiral  
68 cleavage prior to the occurrence of bilateral cleavage. The largest blastomere, 2d,  
69 undergoes four rounds of asymmetric spiral cleavage prior to the bilateral cell  
70 division (Figure 1a-e). The first two rounds of asymmetric cleavage give rise to  
71 two smaller vegetal blastomeres,  $2d^2$  and  $2d^{12}$ , and a larger animal blastomere,  
72  $2d^{11}$  (Figure 1a-b). When  $2d^{11}$  divides the polarity is reversed, and a smaller  
73 animal blastomere ( $2d^{111}$ ) and a larger vegetal blastomere ( $2d^{112}$ ) are generated

74 (Figure 1c). The cell size polarity is again reversed during the next cleavage of  
75  $2d^{112}$ , yielding a smaller vegetal blastomere ( $2d^{1122}$ ) and a larger animal  
76 blastomere ( $2d^{1121}$ ; Figure 1e). Blastomere  $2d^{1121}$  then divides symmetrically to  
77 produce a left ( $2d^{11211}$ ) and right daughter ( $2d^{11212}$ )(Figure 1e).

78           In the present study we investigated how this series of cleavages is  
79 linked with the development of the unique morphology of bivalves. Focusing on  
80 the shell field precursors in bivalve embryos we traced the cell lineages of the  
81 early blastomeres with a fluorescent photoconversion technique using Kaede  
82 fluorescent protein[5].

83

## 84 **2.MATERIALS AND METHODS**

85 Adult specimens of the Japanese purple mussel *Septifer virgatus* (Wiegmann,  
86 1837) were collected in Tsuyazaki, Fukuoka Prefecture, Japan. Induction of  
87 spawning and in vitro fertilization were performed as described in [4]. The  
88 handedness of spiral cleavage was unexpectedly reversed in the eggs from  
89 Tsuyazaki individuals compared with those from Kashima described in  
90 [4](dextral in Kashima [4] and sinistral in Tsuyazaki: this study), and we

91 confirmed that the direction of the spiral cleavage was reversed for all cleavages  
92 up to the bilateral cleavage of 2d<sup>1121</sup> for all specimens examined (Figure 1a-e,  
93 Table 1). This polymorphism in the handedness of spiral cleavage has been  
94 reported in another bivalve species *Dreissena polymorpha*[6].

95 mRNA for Kaede was transcribed from a pBluescript RN3 vector[7], and  
96 Kaede mRNA (3 µg/µl) was injected into fertilized eggs.

97 Kaede fluorescence can be irreversibly converted from green to red by  
98 irradiation with ultraviolet light. Photoconversion was performed using a  
99 confocal laser scanning microscope (CLSM, Zeiss LSM710, Germany) at a 405 nm  
100 wavelength. The laser was applied until we confirmed that sufficient  
101 photoconversion was induced. Among photoconverted embryos, about 20%  
102 showed abnormal morphology at the trochophore stage and were excluded from  
103 our analysis. Swimming larvae were immobilized prior to observation by fixing  
104 with 4% paraformaldehyde and observed by CLSM. The fluorescent signal could  
105 be observed up to 10 h after fixation. It should be noted that some converted cells  
106 appeared yellowish because unconverted green Kaede protein was translated

107 from the injected mRNA even after photoconversion. Unmerged fluorescent  
108 signals are shown in Figure S1.

109

### 110 **3.RESULTS**

111 To confirm that 2d blastomeres contribute shell field precursors, 2d blastomeres  
112 were photoconverted at the nine-cell stage. Following photoconversion of a 2d  
113 blastomere, the converted signal was widely detected in the dorsal region of the  
114 post-trochal epidermis (Figure 2a-c). Importantly, all of the shell field cells were  
115 labeled (Figure 2b, Table 1), indicating that the shell field cells were solely  
116 derived from 2d descendants.

117         Prior to the occurrence of bilateral cleavage, 2d blastomeres undergo four  
118 rounds of asymmetric cleavage to produce four micromeres (Figure 1a-d). These  
119 micromeres were photoconverted after the bilateral cleavage of 2d<sup>1121</sup> because  
120 each blastomere is most easily identified at this stage of development.

121         At this stage, derivatives of 2d<sup>2</sup> have already undergone two rounds of  
122 cell division. We photoconverted all of the derivatives of 2d<sup>2</sup> (Figure 2j). The  
123 converted signal was detected in the left side of both the anterior and posterior of



124 the post-trochal epidermis in these larvae. Importantly, however, the signal was  
125 not detected in the shell field (Figure 2k, Table 1).

126           When 2d<sup>12</sup> was photoconverted, the signal was observed on the right side  
127 of the anterior of the post-trochal epidermis, but no signal was detected in the  
128 shell field (Figure 2l-m, Table 1).

129           When the 2d<sup>111</sup> micromere was photoconverted, the signal was detected  
130 in the anterior dorsal midline of the post-trochal epidermis (Figure 2o-p, Table 1).

131           When 2d<sup>1122</sup> was labeled, the signal was detected in the posterior epidermis  
132 (Figure 2q-r, Table 1). No signal was detected in the shell field in either case (2d<sup>111</sup>  
133 or 2d<sup>1122</sup>).

134           We then photoconverted each bilateral daughter of 2d<sup>1121</sup> to determine  
135 whether the bilateral shell fields differentiate according to the bilateral cleavage  
136 of 2d<sup>1121</sup>. When 2d<sup>11211</sup> (the left side daughter of 2d<sup>1121</sup>) was photoconverted, the  
137 signal was detected not only in the shell field, but also in the surrounding  
138 epidermis (Figure 2d-f). Thus, even at this stage the developmental outcome is  
139 not restricted to the shell field cells. Importantly, the signal was detected not only  
140 in the left side of the shell field, but also in the right side (Figure 2e, Table 1).

141 Interestingly, the signal was biased toward the left posterior in all larvae.  
142 Similarly, when  $2d^{11212}$  (the right side daughter of  $2d^{11211}$ ) was photoconverted, the  
143 signal was observed in both the shell field and the surrounding epidermis (Figure  
144 2g-i, Table 1). The signal in the shell field was biased toward the right anterior of  
145 the shell fields in all larvae.

146           Bivalve shell fields are bilaterally separated by ligament cells that  
147 develop along the dorsal midline (Fig. 1f, g, [3]). Differentiation of the ligament  
148 cells is clearly visible by specific upregulation of the *chitin synthase (cs)* gene  
149 during the trochophore stage[8]. Photoconversion indicated that all of the shell  
150 field cells are derived either from  $2d^{11211}$  or  $2d^{11212}$ . Based on *dpp* expression noted  
151 in oyster embryos, Kin et al.[3] suggested previously that ligament cells are  
152 derived from the descendants of  $1d^{12}$  and  $2d^2$ . Thus, we examined any possible  
153 contribution from the  $1d$  cell lineage, and found that  $1d$  develops into the anterior  
154 epidermis, including the prototroch (Figure S2, Table 1), but not into shell field.  
155 Thus we concluded that the ligament cells are only derived from  $2d^{11211}$  and  
156  $2d^{11212}$ .

157

158 **4. DISCUSSION**

159 In the present study we found that all shell field precursors are derived from  
160  $2d^{1121}$ , although the developmental fate of  $2d^{1121}$  is not restricted to the shell field  
161 cells alone. Importantly, the bilateral shell fields were not derived exclusively  
162 from the daughter cells of  $2d^{1121}$  of each respective side. Instead, the derivatives of  
163 the daughter blastomeres contributed to both sides of the shell field by spreading  
164 across the midline (Figure 1f, g, 2e,h). Thus, our results did not support the  
165 classical hypothesis that the bilaterally separated shell plates of bivalves are  
166 derived from bilateral descendants of  $2d[1]$ . It is notable that descendants of the  
167  $2d$  blastomere also show bilateral cell division in gastropods, as well as in  
168 annelids (e.g., [9-13]), and together with  $4d$ ,  $2d$  was shown to demonstrate  
169 organizing activity in annelids[14]. So it is likely that the bilateral cell division of  
170  $2d$  descendants was established much earlier than the emergence of bivalves,  
171 possibly for the establishment of the bilateral body plan from the spiral  
172 cleavage[15]. The bilateral shell plates, however, might have evolved irrespective  
173 of bilateral cleavage.

174           The innovation of ligament cells in the dorsal midline of the shell field is  
175 critical for the unique body plan of bivalves[16]. Our lineage tracing indicates  
176 that ligament cells differentiate from the 2d<sup>1121</sup> lineage of cells just like other  
177 shell field cells (Figure 1f, g, 2d-i), indicating that the ligament cells emerged as a  
178 subpopulation of shell field cells. The ligament cells are specifically marked by  
179 the upregulation of *cs* [8], and the expression of *dpp* earlier than *cs* [3]. Prior to  
180 shell field invagination, *dpp* is also expressed in cells abutting the shell field  
181 midline, both anteriorly and posteriorly [3]. Although we demonstrated that these  
182 *dpp* positive cells (1d<sup>12</sup> and 2d<sup>2</sup>) do not differentiate into either shell field cells or  
183 ligament cells, it is still possible that *dpp* plays an inductive role in ligament  
184 differentiation. Functional studies of bivalve *dpp* may advance our understanding  
185 of the evolution of the unique bivalve body plan.

186           Innovation of the ligament provided mobility between the separated  
187 shell plates of bivalves, and thus it may have accompanied the evolution of  
188 adductor muscles to open and close the shells. Elucidation of the developmental  
189 mechanism of ligament cells may provide a clue to understanding how the

190 innovation of the ligament and that of adductor muscles are linked during  
191 evolution.

192

193

194 Ethics: Research was carried out according to the university's guideline.

195 Data accessibility: The datasets supporting this article have been uploaded as  
196 part of the supplementary material.

197 Author's contribution: All authors contributed to the design of the study, collection  
198 of data and writing of the article. All authors approve the final version of this  
199 manuscript and agree to be held accountable for all aspects of the work  
200 performed.

201 Competing interests: We declare we have no competing interests.

202 Acknowledgement: We thank Yoshihisa Kurita for providing us purple mussels,  
203 and also for sharing unpublished results.

204 Funding: NH was supported as JSPS pre-doctoral research fellow.

205

## 206 **References**

207 [1] Lillie, F.R. 1895 The embryology of the Unionidae. A study in cell lineage. *J.*  
208 *Morphol.* **10**, 1-100.

209 [2] Meisenheimer, J. 1901 Entwicklungsgeschichte von *Dreissensia polymorpha*  
210 Pall. *Zeitschrift f. wissenschaft. Zoologie* **69**, 1-137.

- 211 [3] Kin, K., Kakoi, S. & Wada, H. 2009 A novel role for *dpp* in the shaping of  
212 bivalve shells revealed in a conserved molluscan developmental program. *Dev.*  
213 *Biol.* **329**, 152-166.
- 214 [4] Kurita, Y., Deguchi, R. & Wada, H. 2009 Early development and cleavage  
215 pattern of the Japanese purple mussel, *Septifer virgatus*. *Zool. Sci.* **26**,  
216 814-820.
- 217 [5] Ando, R., Hama, H., Yamamoto-Hino, M., Mizuno, H. & Miyawaki, A. 2002 An  
218 optical marker based on the UV-induced green-to-red photoconversion of a  
219 fluorescent protein. *Proc. Natl. Acad. Sci. USA* **99**, 12651-12656.
- 220 [6] Luetjens, C.M. & Dorresteijn, A.W. 1995 Multiple, alternative cleavage  
221 patterns precede uniform larval morphology during normal development of  
222 *Dreissena polymorpha* (mollusca, Lamellibranchia). *Roux's Arch. Dev. Biol.* **205**,  
223 138-149.
- 224 [7] Lemaire, P., Garrett, N. & Gurdon, J.B. 1995 Expression cloning of *Siamois*, a  
225 *Xenopus* homeobox gene expressed in dorsal vegetal cells of blastulae and able  
226 to induce a complete secondary axis. *Cell* **81**, 85-94.
- 227 [8] Hashimoto, N., Kurita, Y., Murakami, K. & Wada, H. 2014 Cleavage pattern  
228 and development of isolated D blastomeres in bivalves. *J. Exp. Zool. (Mol. Dev.*  
229 *Evol.)* **324B**, 13-21.
- 230 [9] Conklin, E.G. 1897 The embryology of *Crepidula*. *J. Morphol.* **13**, 3-209.
- 231 [10] Schneider, S.Q. & Bowerman, B. 2007  $\beta$ -catenin asymmetries after all  
232 animal/vegetal-oriented cell divisions in *Platynereis dumerilii* embryos mediate  
233 binary cell-fate specification. *Dev. Cell* **13**, 73-86.

- 234 [11] Meyer, N.P. & Seaver, E. 2010 Cell lineage and fate map of the primary  
235 somatoblast of the polychaete annelid *Captella teleta*. *Integr. Comp. Biol.* **50**,  
236 756-767.
- 237 [12] Chan, X.Y. & Lambert, J.D. 2014 Development of blastomere clones in the  
238 *Ilyanassa* embryo: transformation of the spiralian blastula into the larval body  
239 plan. *Dev. Genes Evol.* **224**, 159-174.
- 240 [13] Lyons, D.C., Perry, K.J. & Henry, J.Q. 2015 Spiralian gastrulation: germ  
241 layer formation, morphogenesis, and fate of the blastopore in the slipper snail  
242 *Crepidula fornicata*. *EvoDevo* **6**, 24.
- 243 [14] Nakamoto, A., Nagy, L.M. & Shimizu, T. 2011 Secondary embryonic axis  
244 formation by transplantation of D quadrant micromeres in an oligochaete  
245 annelid. *Development* **138**, 283-290.
- 246 [15] Lyons, D.C., Perry, K.J., Lesoway, M.P. & Henry, J.Q. 2012 Cleavage pattern  
247 and fate map of the mesentoblast, 4d, in the gastropod *Crepidula*: a hallmark  
248 of spiralian development. *EvoDevo* **3**, 21.
- 249 [16] Owen, G., Trueman, E.R. & Younge, C.M. 1953 The ligament in the  
250 Lamellibranchia. *Nature* **171**, 73-75.
- 251
- 252

253 **Figure legends**

254 **Figure 1. Schematic illustration of the cleavage pattern and cell lineage mapping**  
255 **of 2d descendants.**

256 (a-e) Schematic illustration of the cleavage pattern of 2d descendants. (f) Summary  
257 of the cell lineage mapping of the 2d descendants in trochophore larva. Dorsal  
258 views, anterior to the top. (g) Tree diagram of the cell lineage and developmental  
259 fate of 2d descendants.

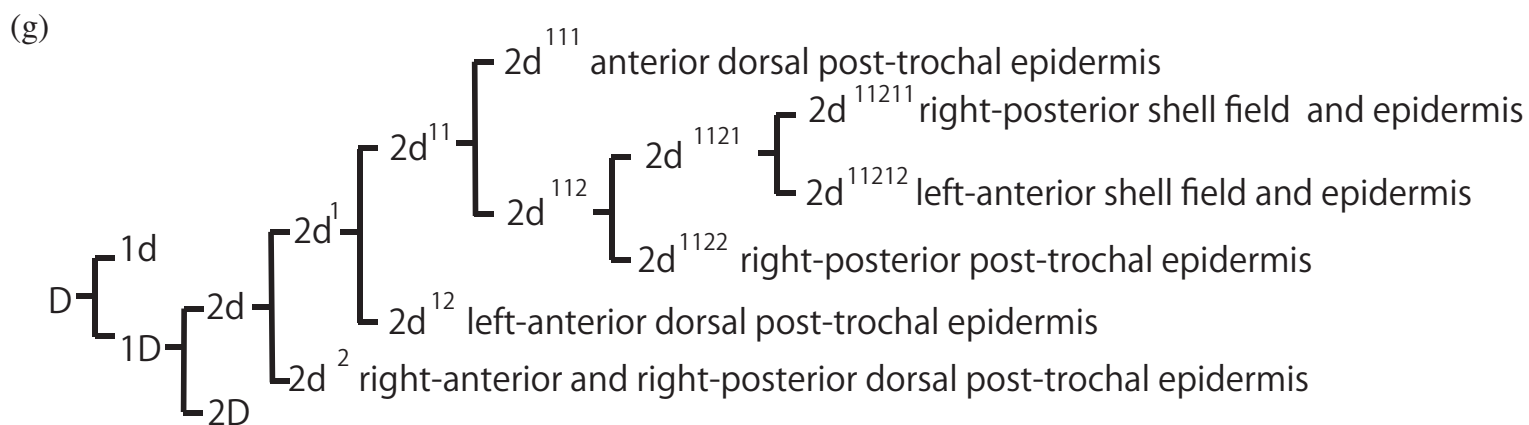
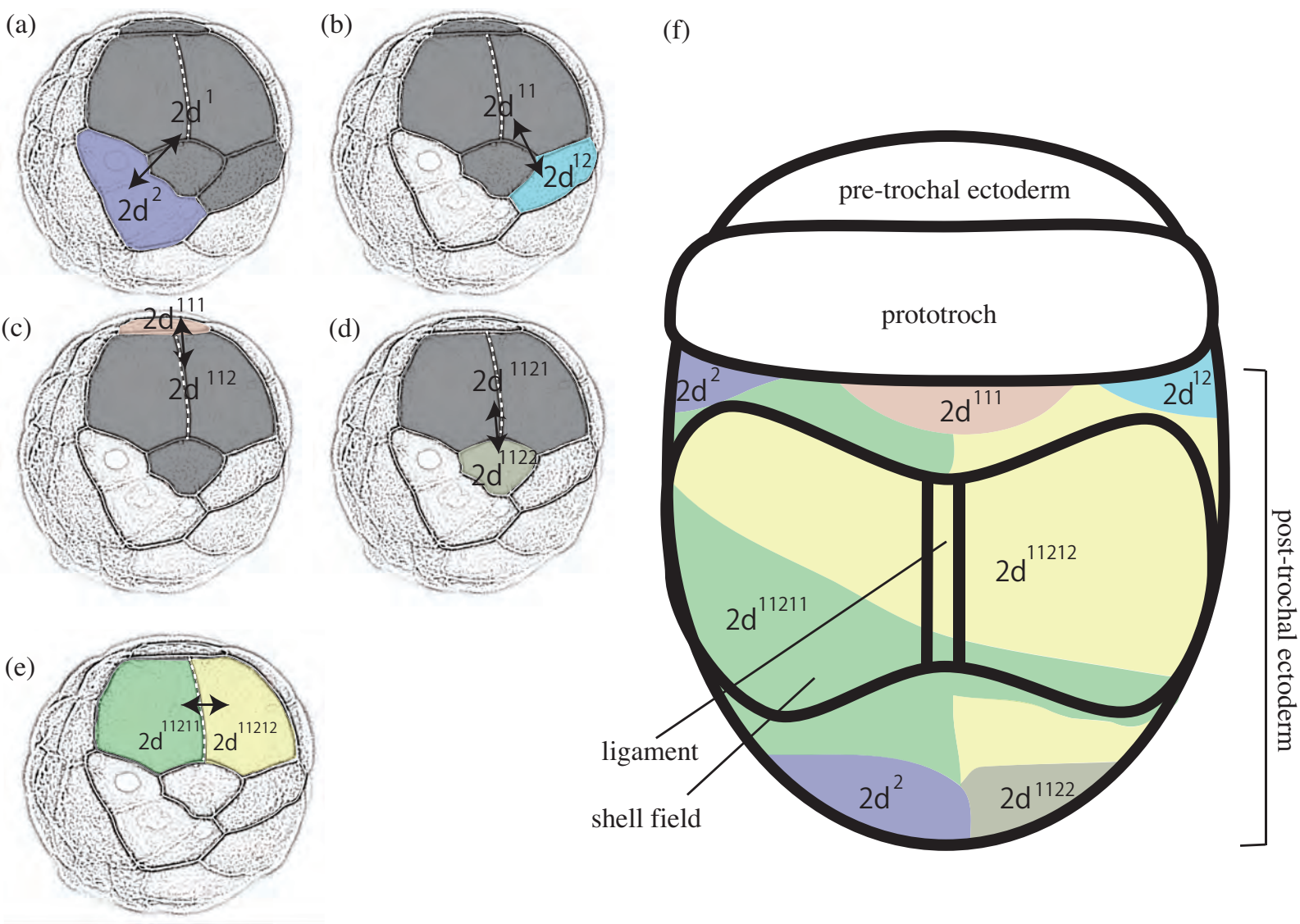
260

261 **Figure 2. Cell lineage tracing of 2d and descendant blastomeres.**

262 (a-c) Cell lineage of 2d. Kaede was converted at 9 cell stage (a: view from right  
263 side), and the fate of 2d was observed at trochophore stage (b-c). (d-r) Cell lineage  
264 of  $2d^{11211}$  (d-f),  $2d^{11212}$  (g-i),  $2d^2$  (j-k),  $2d^{12}$  (l-m),  $2d^{111}$  (o-p) and  $2d^{1122}$  (q-r). Noted that  
265 some converted cells appeared yellowish because unconverted green Kaede  
266 protein was translated from the injected mRNA even after photoconversion.  
267 Shell field boundary is indicated by broken line. Anterior to the top except for (o)  
268 in which ventral to the top. Scale bars: 50  $\mu$ m.

269





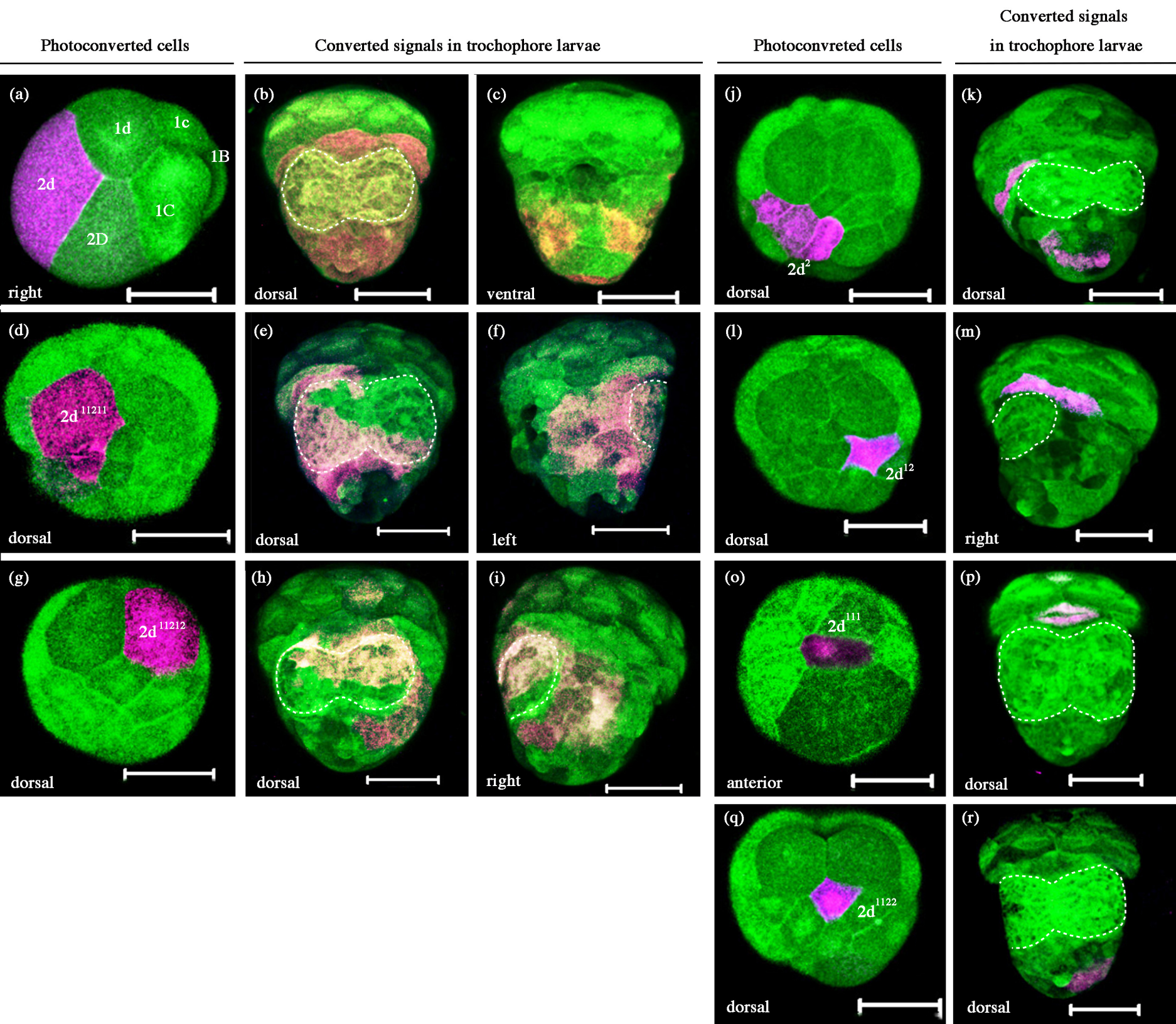


Table 1. Cell lineage of 2d descendants

photoconverted cells	developmental fate at trochophore stage	no. larvae showing the fate / no. embryos observed	Figure
2d	dorsal post-trochal epidermis and shell field	4/4	2a-c
2d2	right-anterior and right-posterior dorsal post-trochal epidermis	8/8	2j-k
2d12	left-anterior dorsal post-trochal epidermis	6/6	2l-m
2d111	anterior dorsal post-trochal epidermis	6/6	2o-p
2d1122	right-posterior post-trochal epidermis	7/7	2q-r
2d11211	right-posterior shell field and ligament	8/8	2d-f
2d11212	left-anterior and posterior dorsal post-trochal epidermis	9/9	2g-i
1d	prototroch and pre-trochal epidermis	4/4	S1